Analysis of *Chlamydomonas* SF-assemblin by GFP tagging and expression of antisense constructs

Karl-Ferdinand Lechtreck*, Jutta Rostmann and Andrea Grunow

Botanisches Institut, Universität zu Köln, Germany

*Author for correspondence (e-mail: karl.lechtreck@uni-koeln.de)

Accepted 6 January 2002

Journal of Cell Science 115, 1511-1522 (2002) © The Company of Biologists Ltd

Summary

Striated fiber assemblin (SF-assemblin or SFA) is the major component of the striated microtubule-associated fibers (SMAFs) in the flagellar basal apparatus of green flagellates. We generated nuclear transformants of *Chlamydomonas* expressing green fluorescent protein (GFP) fused to the C-terminus of SFA. SFA-GFP assembled into striated fibers that exceeded those of wild-type cells in size by several fold. At elevated temperatures (≥32°C) SFA-GFP was mostly soluble and heat shock depolymerized the SMAFs. C-terminal deletions of 18 or only six residues disturbed the ability of SFA-GFP to polymerize, indicating an important role of the C-terminal domain for fiber formation. The exchange of the penultimate Ser275 with alanine made SFA-GFP highly insoluble, causing aberrant fiber formation and conferring heat stability to the fibers. By contrast, a replacement with glutamic acid increased the solubilty of the molecule, indicating that phosphorylation on Ser275 might control solubility of SFA. In vivo observation of GFP fluorescence showed that SFA-GFP fibers were disassembled during mitosis. In cells overexpressing full-length or truncated SFA-GFP, the amount of wild-type protein was reduced. Elevated temperatures dissolved SFA-GFP fibers and induced the synthesis of SFA, suggesting that cells control both the amount of soluble and polymeric SFA. By expressing constructs consisting of cDNA and genomic DNA for parts of SFA in antiparallel configuration, the amount of SFA was severely reduced. In these strains we observed defects in flagellar assembly, indicating an important role for noncontractile striated roots in the flagella apparatus.

Movies available on-line

Key words: Coiled-coil, Flagella, RNAi, Striated roots, Microtubule

Introduction

The eukaryotic flagellar apparatus commonly consists of the protruding flagellum and the flagellar basal apparatus, a cytoskeletal complex that organizes and anchors the flagellum. The ultrastructure of the flagellar basal apparatus varies considerably among species and cell types. Microtubules surround the basal bodies in various patterns and the basal bodies are attached to a variety of fibrous structures (Pitelka, 1969). Immunological and biochemical analyses indicated that the fibrous elements in the basal apparatus are heterogeneous in composition but, in protists, at least two common types have been identified, namely striated fiber assemblin (SFA)- and centrin-fibers. The latter are contractile and include connections between basal bodies or between basal bodies and the cell nucleus. Centrin and centrin homologues were also observed in the lumen of basal bodies and centrioles, at spindle poles or in the half bridge of the yeast spindle pole body, suggesting a broad range of functions for this calcium-binding protein (Schiebel and Bornens, 1995). The second class of fibrous elements in the basal apparatus includes the microribbons of *Giardia*, the kinetodesmal fibers of ciliates and the green algal SMAFs (striated microtubule-associated fibers) (Holberton et al., 1988; Sperling et al., 1991; Lechtreck and Melkonian, 1991). These fibers are noncontractile, narrowly striated (~30 nm axial repeat) and often attached to microtubules (reviewed by Lechtreck and Melkonian, 1998). Although microribbons and kinetodesmal fibers are complex in composition (consisting of several proteins of ~30 kDa), SMAFs can be assembled in vitro solely from the 34 kDa protein SFA, making them an ideal system to study noncontractile striated fibers. In *Chlamydomonas* and other green flagellates, the SMAFs form a cross-like pattern and run alongside the proximal parts of the four bundles of flagellar root microtubules.

Striated fiber assemblins from flagellate green algae are about 20% identical to β-giardin, one of the proteins in the microribbons (Weber et al., 1993). Both proteins share a similar domain structure with a short, nonhelical, proline-rich head domain and a coiled-coil domain of approximately 250 residues. Striated fiber assemblin is phosphorylated in vivo and the head domain of green algal SFAs contains several potential phosphorylation sites for the $p34^{cdc2}$ kinase. It is not known whether phosphorylation at these sites is responsible for the disassembly of the SMAFs observed during mitosis (Lechtreck and Silflow, 1997). The rod domain of β-giardin/SFA is characterized by a distinctive series of heptads arranged into blocks of four, followed by a skip residue interrupting the heptad pattern (Holberton et al., 1988; Weber et al., 1993). A study of the in vitro assembly properties of *Chlamydomonas*-SFA showed that headless molecules were assembly incompetent, whereas large deletions and insertions in the rod domain were tolerated and resulted in a shift in the axial repeat of the striated fibers (Lechtreck, 1998). SFA polymers are polar and consist of 2 nm protofilaments that are thought to be composed of parallel dimers overlapping with the N- and C-

terminal parts of their rod domains (Patel et al., 1992; Lechtreck, 1998).

Because SMAFs and similar fibers are rigid, they are thought to function as stabilizing elements in the basal apparatus. Noncontractile striated fibers, often with differing periodicities to the SMAFs, have been described in a broad range of organisms, including mammals, suggesting that these fibers have an important function in the basal apparatus. Detailed studies on in vivo function of SMAFs and similar roots are lacking, mainly because of the absence of mutants with defects in these fibers. Here, we present in vivo data on the expression of green fluorescent protein (GFP)-tagged SFA molecules and the repression of SFA expression by RNA interference. Our results indicate that the amount of SFA in *Chlamydomonas* is controlled by a complex mechanism balancing synthesis, degradation and polymerization of the protein, and that SMAFs are needed for correct flagellar assembly.

Materials and Methods

Cell culture

Chlamydomonas reinhardtii strain CC-3395 (cwd, arg7.8) was maintained in TAP media supplemented with 0.02% ariginine in batch cultures (Gorman and Levine, 1965). If not otherwise noted, cells were maintained in a light:dark cycle of 14:10 hours and at 25°C. Onset of light was at 6 o'clock Middle European Summer Time (MESZ) and experiments were performed or started during the first six hours of the light phase. In heat-shock experiments cells were allowed to recover at room temperature unless otherwise indicated. All in vivo observation were carried out at room temperature.

Plasmids and transformation

A genomic library of *Chlamydomonas* (Schnell and Lefebvre, 1993) was screened using a cDNA-clone coding for SFA of *C. reinhardtii* (or CRA8) (see Lechtreck and Silflow, 1997). The screen resulted in three clones (BA1, BA5 and BA10); BA1 was used as a template for subsequent PCR reactions. The coding region of SFA including 88 bp of the 5′-UTR was amplified using Taq polymerase (GeneCraft, 488163 Münster, Germany), a forward primer UTRf4 (5′-GCGTCTAGAGCTAGTTCTCATACATATTACTC-3′), which contained an overhanging *Xba*I site followed by a *Nhe*I site, and the backward primer GFPr1 (5′-GCTCTAGAGCTGCGCTGACCAGCT-TGAGG-3′), which contained a *Xba*I site, omitted the stop codon of SFA and adjusted the reading frame to that of GFP. The 2.2 kb product was digested with *Xba*I and ligated into pCr-GFP (BioCAT, Heidelberg, Germany) (Fuhrmann et al., 1999), which contained a synthetic *gfp*-gene codon-adjusted for *Chlamydomonas* and the 3′ UTR of the *rbcS2* gene as a terminator sequence. A clone (pCr-SFA-GFP2) containing the *sfa* gene in the correct orientation was partially sequenced, digested with *Nhe*I and *Eco*RI, and the fragment containing the *sfa::gfp::rbcS2* gene was ligated into pCB740 (Schroda et al., 2000) digested with *Nhe*I and *Eco*RI to remove the *hsp70A* gene. Thus, the GFP-tagged *sfa* gene was downstream of the strong HSP70B/rbcS-fusion promoter in a vector containing also the *arg7* gene, a selectable marker for transformation into arginine-requiring strains. The plasmid pCB740-SFA-GFP was linearized with *Eco*RI and transformed into *Chlamydomonas* CC3395 using the glass bead method (Kindle, 1990). A gene coding for SFA with a C-terminal truncation of 18 residues was constructed similarly using the reverse primer GFPr2 (5′-GCTCTAGACCTGCACGATCTCGTCGTCCTC-3′). Constructs with single-residue exchanges or a deletion of six residues were performed accordingly. As a control we used a cell line transformed with pCB740 digested with *Nhe*I and *Eco*RI.

To obtain the antisense gene *AS1*, parts of the genomic clone BA1 and the cDNA clone CRA8 were amplified using the primers f1UTR (5′-CGCGCATGCTAGCTTCTCATACATATTACTC-3′) and r1AS (5′-GCGTCTAGACGTTCGGTGACATGCTCAAGC-3′) containing a *Sph*I and a *Xba*I site, and primers f1AScDNA (5′-GCGGATC-CTTCTCATACATATTACTC-3′) and r1AS containing a *Bam*HI and *Xba*I, respectively. After digestion with the enzymes indicated, the two fragments of ~350 and 200 bp were ligated into pCr-GFP digested with *Sph*I and *Bam*HI, which removed the *GFP* gene. The resulting plasmid was digested with *Sph*I and *Eco*RI and the fragment containing the AS1 construct was ligated into pCB740 downstream of the HSP70B/rbcS2 promoter. Double transformants were obtained by cotransformation of AS5 with pCB740-SFA-GFP and the pJN4 plasmid (Nelson et al., 1994).

Western blotting analysis

Chlamydomonas cells, 10 ml, were pelleted at 500 ***g*** for 3 minutes, resuspended in 500 µl MT buffer, and lysed by the addition of 500 µl MT/3% Triton X-100. Cytoskeletons were immediately pelleted at 15.300 ***g*** and 200 µl of the supernatant were precipitated with 1.4 ml of methanol at –20°C for several hours. Whole cells were pelleted for 2-4 minutes at full speed in a table-top centrifuge. All pellets were boiled in 2× sample buffer, subjected to SDS-PAGE and transferred onto PVDF membrane. Western blotting was carried out as described previously (Lechtreck and Geimer, 2000) and blots were documented using a digital camera. Cycloheximide (Sigma) was used at 2 µg/ml and removed by repeated washes (3×) in culture medium (500 ***g***, 5 minutes).

Nothern blotting

Total RNA was isolated from frozen cells (–80°C) using a guanidine thiocyanate-phenol solution and precipitation with LiCl (Ausubel et al., 1995), separated by denaturating agarose electrophorese, and transferred to Biodyne B membrane (PALL, Dreieich, Germany). Probes (*Hin*dIII fragment of pQE-SFA or *Sph*I/*Bam*HI fragment of pCR-AS1) were labeled with ^{32}P-ATP by random oligonucleotide-primed synthesis using the Klenow fragment of DNA polymerase I. For northern hybridization, we followed the protocol of Church and Gilbert (Church and Gilbert, 1984) and membranes were scanned using a PhosphorImager (Storm).

Antibodies and microscopy

The following antibodies were used for western blotting (WB), indirect immunofluorescence (IF) and immunogold electron microscopy (EM): polyclonal anti-SFA (WB 1:2000-5000, IF 1:100-200, EM 1:200) (Lechtreck, 1998), monoclonal anti-centrin BAS6.8 (WB 1:50), polyclonal anti-GFP 290 (WB 1:3000, EM 1:100, Abcam, Cambridge, UK), monoclonal anti-acetylated tubulin 6-11B-1 (IF 1:400, Sigma) and monoclonal anti-α-tubulin (IF 1:400, clone DM 1A, Sigma). Secondary antibodies were obtained from Dianova (anti-rabbit-IgG-Cy3, anti-mouse-IgG-Cy3; Hamburg, Germany), Sigma (anti-rabbit-IgG-FITC, anti-rabbit or anti-mouse-IgG conjugated to alkaline phosphatase) or British BioCell (anti-rb-IgG 10-nm gold; Cardiff, UK) and used as recommended by the manufacturer.

For fluorescence microscopy and indirect immunofluorescence, *Chlamydomonas* cells were immobilized on poly-L-lysine-treated slides and submerged in methanol at –20°C for 10-25 seconds. Cytoskeletons were isolated by detergent treatment (1.5% Triton X-100) in MT buffer (30 mM Hepes, 15 mM KCl, 5 mM, $MgSO_4$, 5 mM EGTA, pH 7) as described previously (Lechtreck and Geimer, 2000). Cells were observed and documented using a Nikon Eclipse E800 equipped with a RT monochrome Spot camera (Diagnostics Instruments). Images were captured using Metamorph, converted to 8-bit, exported to Photoshop (Adobe) and mounted with Adobe

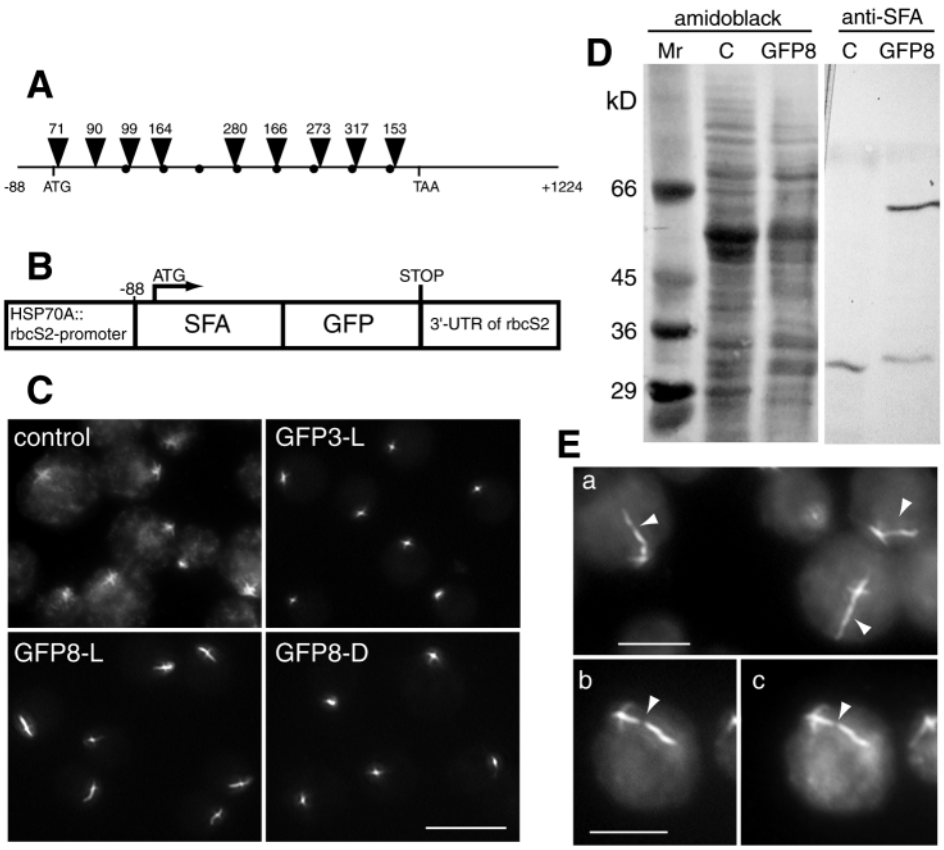

Fig. 1. Analysis of *Chlamydomonas* cells expressing GFP-tagged SFA. (A) Gene structure of *sfa* (accession number AJ344366). The size and positions of the introns are indicated. The positions of the codons of the skip residues are marked by dots. Note the regular spacing of the introns. (B) Gene construct used for the expression of SFA-GFP. The arrow indicates the position of the start of translation. (C) Comparison of the SMAFs in control cells (control; anti-SFA staining) with the GFP signals observed in GFP3 and GFP8. Cells were fixed with methanol (–20°C) for 20 seconds. GFP3 expressed moderated amounts of SFA-GFP, forming cross-like structures similar to that observed in control cells by indirect immunofluorescence, whereas GFP8 cells overexpressed SFA-GFP, causing oversized fibers, when cultivated with a light/dark-cycle of 14/10 hours (GFP3-L and GFP8-L). Small fibers were present in GFP8 when cultivated in the dark for 2 days (GFP8-D). Bar, 10 μm. (D) Western blot of control (C) and GFP8 cells. The membrane strip on the left was stained with amidoblack and the positions of the standard proteins (Mr) are indicated on the left. Anti-SFA reacted with a band of 34 kDa in control and GFP8 cells, and a band of approximately 60 kDa in GFP8. (E) Details of strain GFP8. (a) Frequently one (indicated by arrowheads) of the four SFA-GFP fibers was much longer than the other three. (b,c) GFP signal (b) or indirect immunofluorescence with anti-SFA (c) of a GFP8 cell with a gap in one of the SFA-GFP fibers. Bars, 5 μm.

Illustrator. For in vivo observations, *Chlamydomonas* cells were immobilized in TAP/0.75-1.5% low melting agarose, adopted from a previously described method (Reize and Melkonian, 1989). All methods for standard or postembeddding immunogold electron microscopy have been previously described (Lechtreck and Geimer, 2000).

Results

GFP tagging of *Chlamydomonas* SFA

A cDNA clone coding for SFA (CRA8) (Lechtreck and Silflow, 1997) was used to screen a genomic library of *Chlamydomonas*. Three clones resulted (BA1, BA5 and BA10), all containing the complete coding region of SFA. The sequence contained nine introns, seven of which were located in the sequence coding for the rod domain near (≤11 bp) the codons of the skip residues (Fig. 1A). We constructed a plasmid (pCB740-SFA-GFP) containing the *sfa::gfp* gene downstream of the HSP70B/rbcS2 fusion promoter and upstream of the rbcS2 terminator sequence (Fig. 1B) (Schroda et al., 2000). Transformants were analyzed by fluorescence microscopy and western blotting of whole cells, and in about one third of the analyzed transformants (n=32) SFA-GFP was detected. Some strains (e.g. GFP8) contained considerably more tagged than wild-type protein and therefore the resulting polymers were named SFA-GFP fibers to distinguish them form SMAFs assembled from wild-type SFA. Southern blotting showed that GFP8 contained a single copy of pCB740-SFA-GFP (not shown).

SFA-GFP assembled into striated fibers

Fluorescence microscopy revealed that SFA-GFP assembled into cross-like structures centered at the basal bodies (Fig. 1C). In some strains (e.g. GFP3) the size of the cross was similar to that visible in control cells after staining with anti-SFA (~1 μm length) but, in GFP8, one or two branches of the cross were much longer and up to 4 μm in length (Fig. 1C,E). Often, GFP8 cells developed one especially long fiber. These were often irregular in thickness and even had discontinuities in them – breaks that were not bridged by wild-type SFA (Fig. 1Ea-c). In western blots using anti-SFA, the GFP-tagged protein was visible in isolated cytoskeletons as one or several bands at approximately 60 kDa, in addition to the 34 kDa band representing SFA (Fig. 1D).

Chlamydomonas SMAFs run along the four bundles of microtubular flagellar roots, which, in contrast to the other cytoskeletal microtubules, contain acetylated tubulin (Fig. 2, top) (LeDizet and Piperno, 1986). The SMAFs along the two-stranded bundles sit end-to-end and were originally described as one continuous fiber, whereas those along the four-stranded roots sit laterally on the axis forming fibers (Fig. 5a,b) (Goodenough and Weiss, 1978; Weiss, 1984). The length of the proximal acetylated region of the four microtubular roots

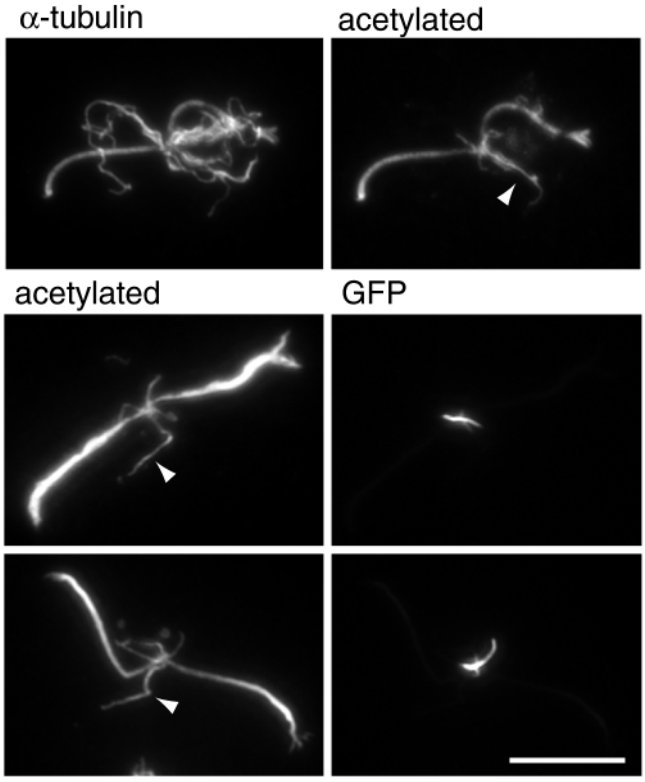

Fig. 2. Analysis of GFP8 cells with antibodies for acetylated tubulin. Top: isolated cytoskeleton of a control cell stained with polyclonal anti-α-tubulin and 6-11B-1 (acetylated tubulin), revealing the numerous microtubules of the cytoskeleton and the four acetylated flagellar roots. Bottom: GFP8 cytoskeletons stained with 6-11B-1 and corresponding GFP images, revealing that prominent SFA-GFP fibers were mostly associated with microtubular bundles characterized by short acetylated regions. The arrowheads mark microtubular roots acetylated over most of their length. Bar, 10 μm.

differed and the prominent fluorescent fibers in GFP8 cells were attached to the roots with short acetylated regions (Fig. 2), with the longest branch mostly (>90%, *n*=30) associated with the root having the shortest acetylated region. Standard electron microscopy showed that GFP8 contained striated fibers, especially along the two-stranded microtubular roots, which exceeded control SMAFs by several fold in length, thickness and width (Fig. 3d-f,h). The cross-striation periodicity of the SFA-GFP fibers was determined with 27.5 nm (*n*=5) similar to that of wild-type SMAFs (27.8 nm in whole mount microscopy) (Lechtreck, 1998). We were able to decorate the fibers with anti-SFA and anti-GFP in immunogold electron microscopy (Fig. 3a-c), confirming that SFA-GFP assembled into microtubule-associated striated fibers. Thin sections of GFP8 frequently showed microtubules radiating from the oversized SMAFs (Fig. 3d,e,h) and emphasized the close association of SMAFs and probasal bodies (Fig. 3f,h).

Heat shock induced disassembly of SFA-GFP fibers

Expression of SFA-GFP was controlled by the strong, constitutive HSP70B/rbcS2 fusion promoter, the activity of which can be modulated by heat shock or culture conditions (Schroda et al., 2000). In fact, the size of the fluorescent fibers was reduced when GFP8 cells were cultivated in the dark for 48 hours (Fig. 1C). Also, signal strength decreased in cultures of high cell density (not shown) and therefore all experiments were carried out with cultures $\leq 10^6$ cells/ml. Heat shock (60 minutes at 40°C) caused the disassembly of the SFA-GFP fibers, with the exception of a dot-like core region near the basal bodies (Fig. 4A, T60). A similar SFA-GFP core structure was also observed in dividing cells when SFA fibers were largely disassembled (see below). Anti-SFA staining of cells after heat shock revealed fibers exceeding the corresponding GFP signals in size, indicating that remnant wild-type SFA fibers were present after heat shock (Fig. 4C). Reassembly of the SFA-GFP fibers was evident 1 hour after the heat shock, when we observed up to four thread-like extensions of the central bright dot (Fig. 4A, T120). These thin fibers became longer and thicker and after 5-6 hours reached the size of those in untreated controls. Heat shock also induced the formation of globular SFA-GFP aggregates in *Chlamydomonas*. These were transient in nature, visible in phase contrast microscopy (Fig. 4A, T240) and often located at the ends of the two long SFA-GFP fibers (Fig. 4A, T240). The proportion of cells with aggregates post heat treatment varied between experiments (not shown). Using cells immobilized in low-melting agarose, it was possible to observe fiber disassembly and reassembly in living cells (Fig. 4B). After heat shock, Schroda et al. (Schroda et al., 2000) observed a strong increase in the amount of mRNA and protein from genes expressed under the control of the HSP70A/rbcS2 fusion promoter. On northern blots probed with a partial cDNA of SFA, a transcript of approximately 3.2 kb and several smaller transcripts were abundant in a GFP8 sample taken 45 minutes after heat shock, whereas these transcripts were not detected in GFP8 cells before or 3 hours after heat shock or in the control strain (Fig. 4D). Despite this obvious increase in the amount of mRNA coding for SFA-GFP, the amount of protein detected on western blots of whole cells showed only minor variations during heat shock (Fig. 4E, top). Fractionation of cells after heat shock confirmed the heat instability of SFA-GFP fibers: SFA-GFP increased in the soluble fraction but was largely removed from the cytoskeletal fraction (Fig. 4E, middle). During recovery, the amount of SFA-GFP in the cytoskeletons increased again. In heat-shocked control cells the amount of SFA showed only minor variations (Fig. 4E, top and bottom). Often, SDS-PAGE revealed a shift in the apparent molecular weight between the soluble and insoluble forms of SFA-GFP and SFA (Fig. 4E), suggesting that a modification like phosphorylation could be responsible for dissolving SFA fibers. Further, anti-SFA detected additional bands near 60 kDa in some westerns (Fig. 4E; Fig. 8A,B), which were also present when protease inhibitors had been added during cell lysis and could be caused by phosphorylation.

Analysis of SFA-GFP in dividing cells

The distribution of SFA during the cell cycle of *C. reinhardtii* has been studied previously by indirect immunofluorescence. Briefly, two of the four SMAFs disassemble prior to mitosis. The remaining fibers fall apart and are then reduced to dot-like structures. One or two dots positive with anti-SFA were present at each spindle pole and in telophase one prominent fiber was formed before the small cross-like structure typical for cells in interphase was re-established (Lechtreck and Silflow, 1997).

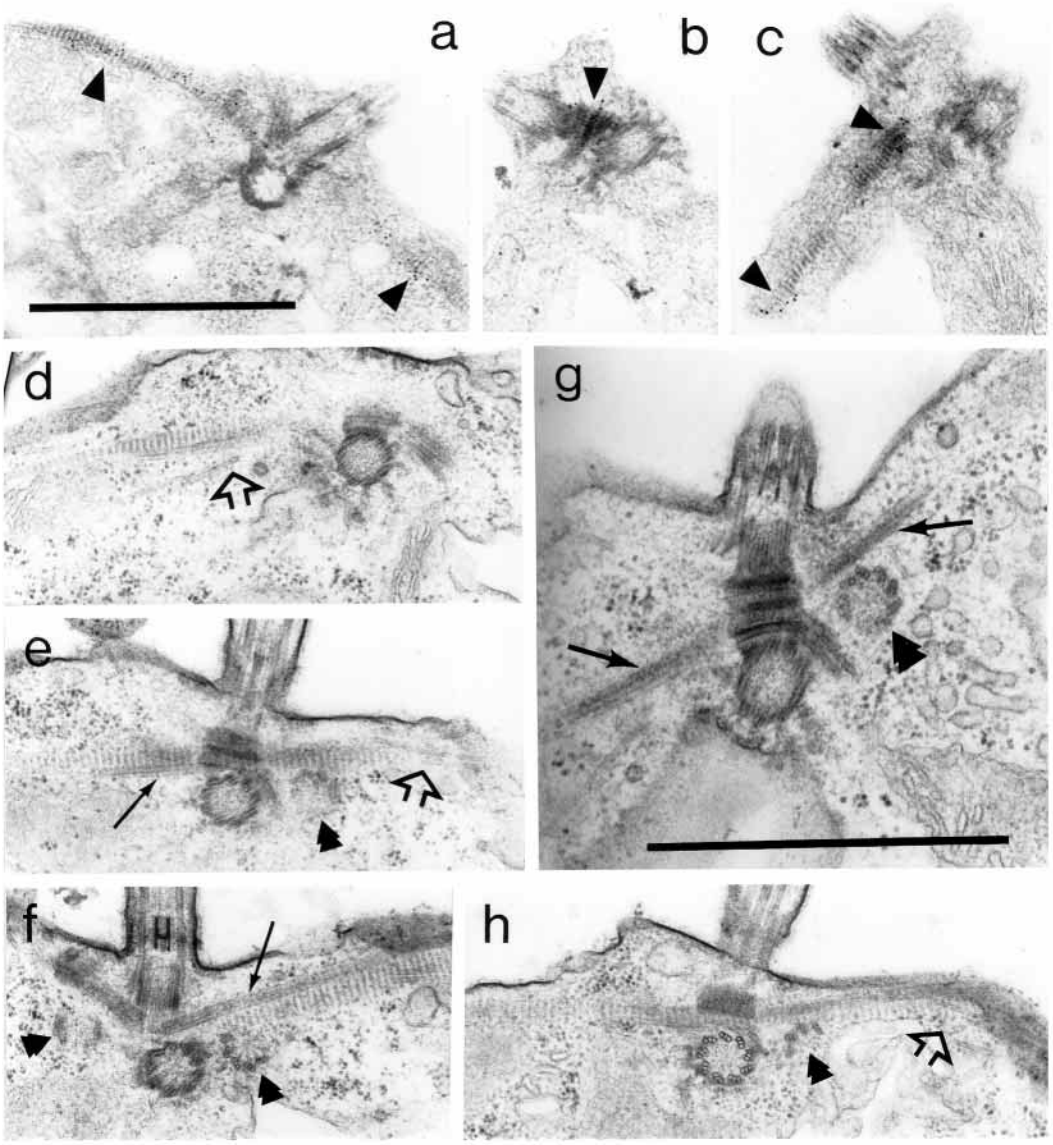

Fig. 3. Analysis of GFP8 cells by standard and immunogold electron microscopy. (a-c) Postembedding immunogold electron microscopy. Sections were stained with anti-rabbit-IgG 10 nm gold and either anti-SFA (a) or anti-GFP (b and c, which are consecutive sections). Arrowheads in a and c show SMAFs, and arrowheads in b indicate the immunodecorated region between the two basal bodies at the origin of the SMAFs. (d-f) Three consecutive sections showing a basal apparatus with prominent SMAFs. Open arrows: microtubules originating on or near the SMAFs; arrows: two-stranded microtubular roots alongside the SMAFs; double arrowheads: new basal bodies. (g) Control cell showing new basal bodies (double arrowhead) and thin SMAFs (arrows), visible as electron-opaque bands along the microtubular roots. For better images of wild-type SMAFs see Goodenough and Weiss (Goodenough and Weiss, 1978). (h) Section through a GFP8 cell with prominent SMAF, secondary cytoskeletal microtubules (open arrow) and new basal body (double arrowhead). Bars, 1 μm.

During mitosis SFA-GFP fibers were disassembled (Fig. 5b, living cells), but we noted that SFA-GFP was removed more rapidly from the fibers along the two-stranded roots than SFA. Furthermore, the remaining dot-like signals contained only small amounts of SFA-GFP, whereas brighter signals were observed after antibody staining (Fig. 5, methanol-fixed cells). To analyze living cells embedded in agarose, we mostly used short exposure times (<1 second), 4× to 16× excitation filters to prevent photodamage, and controlled so that the contractile vacuoles were pumping rapidly indicative for cell viability (Fig. 5e, top). Before mitosis we observed changes in the angle between the SFA-GFP fibers (Fig. 5a, top). Then, the fibers separated and disassembled (Fig. 5b, top). Towards the end of the first division the distance between the dot-like structures present at the apex of both cell halves decreased and often, additional dots appeared (Fig. 5c,d, top). These were either positioned near the cell apex and thus might be located in the duplicated basal apparatus, or deeper in the cell body. Some of these dot-like structures moved with a velocity of up to 0.4 μm/minute. Similar dots were observed previously in control cells (Lechtreck and Silflow, 1997).

The C-terminal domain of SFA is essential for fiber formation

On the basis of the observation that heat shock largely dissolved SFA-GFP fibers, we assumed that the GFP-tag deformed the C-terminus of the protein and thereby destabilized the striated fibers. Attempts to extract SFA-GFP in vitro from isolated cytoskeletons by heat treatment were not successful, indicating that fiber disassembly depended on cellular activities. To examine further the role of the C-terminus in fiber stability, we constructed a GFP-tagged SFA with a C-terminal deletion of 18 residues (SFAΔC18-GFP) (Fig. 6A). In overexpressing strains, for example, ΔC18-11 cells, weak green fluorescence was only detected in a dot-like region near the basal bodies (Fig. 6B). Wild-type SFA was largely insoluble, whereas full length SFA-GFP was present in both the cytoskeletons and the supernatant (Fig. 6C). Densitometric analysis of western blots stained with anti-SFA indicated that about 60% of the total SFA-GFP was insoluble in cells cultivated at 25°C. By contrast, western blot analysis of ΔC18-11 after cell fractionation showed that SFAΔC-GFP was mostly soluble (Fig. 6C). The results suggested that the C-terminal domain of SFA is

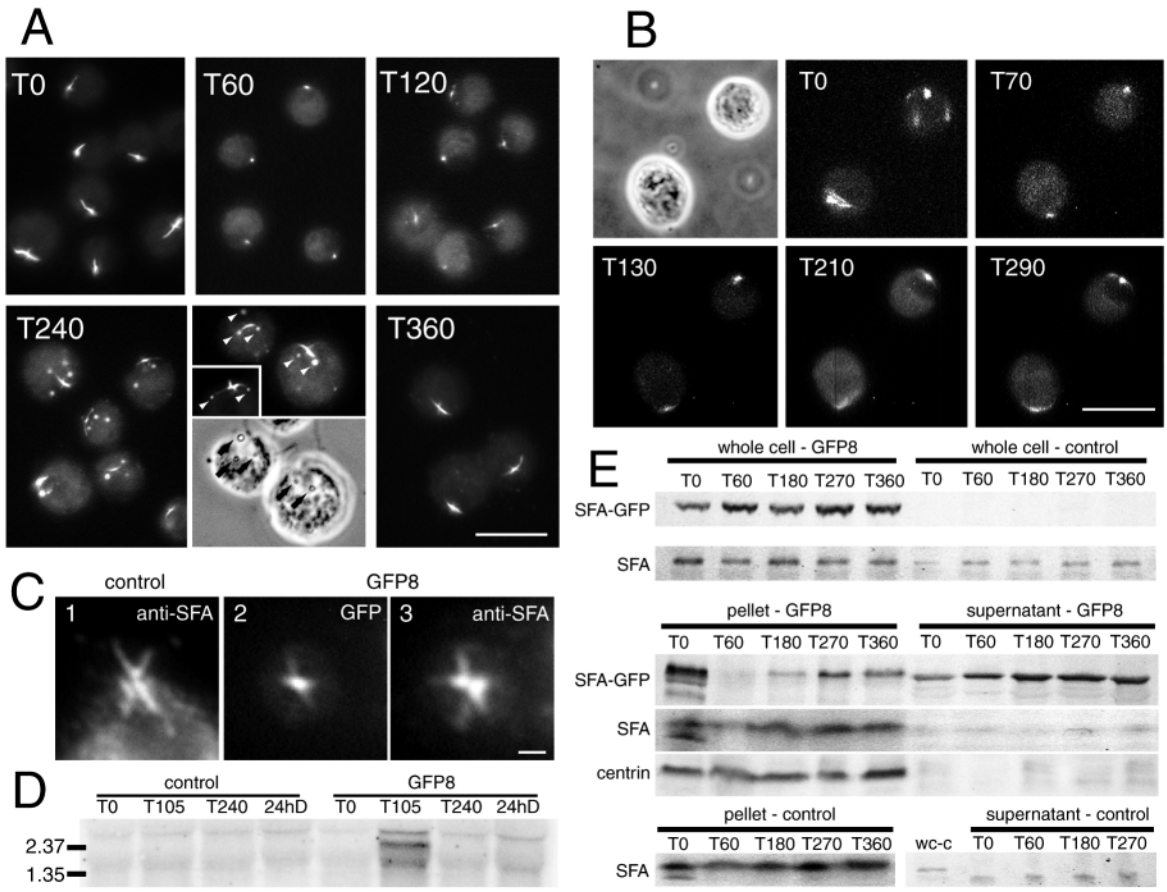

Fig. 4. The effect of heat shock on GFP8 and control cells. (A) A heat shock of 40°C was applied for 60 minutes. Cells were immobilized on slides and fixed by rinsing in –20°C methanol for 20 seconds. T0, cells before heat shock; T60, cells after heat shock. SFA-GFP fibers were largely depolymerized with the exception of a dot-like region near the basal bodies. T120, thin fibers extend from the brighter dot; T240, globular aggregates have formed, in addition to the cross-like structure. These aggregates were also visible in phase contrast (arrows) and were often located at the end of the developing SFA-GFP fibers (insert). T360, SFA-GFP fibers were reassembled almost completely. Bar, 10 μm. (B) In vivo observation of cells embedded in agarose during heat shock and recovery. Each picture represents an average of several images taken at six to seven different focus levels over a period of 5-6 seconds. For heat treatment the slide with the embedded cells was incubated on a temperature-controlled metal block. T0, embedded cells were still able to rotate, causing the SMAFs to appear several times on the averaged image. T70, cells have resorbed the flagella and the fibers were depolymerized. T130, T210, T290, repolymerization of SMAFs first visible as thread-like extensions from the stable core region. Bar, 10 μm. (C) Immunofluorescence analysis of heat-shocked control (1) and GFP8 cells (2, 3) using anti-SFA. (1) In control cells, SMAFs seem to be unaffected by heat shock. (2) GFP fluorescence and corresponding antibody staining (3) of a GFP8 cell after heat shock. The resulting signals show differences in shape and size, indicating an unequal distribution of wild-type and GFP-tagged protein. It should be noted that anti-SFA binds both SFA and SFA-GFP (compare also Fig. 5, bottom). Bar, 1 μm. (D) Northern blot of control and GFP8 cells using a partial cDNA of SFA as a probe. In GFP8 cells, several transcripts at and below ~3.2 kb were detected 45 minutes after heat shock (T105), which were not present before (T0) or three hours after heat shock (T240), or in control cells. 24hD, RNA from cells cultivated in the dark for 24 hours. 30 μg of total RNA were loaded in each lane. The positions of RNA standard molecules are indicated. (E) Western blot analysis of GFP8 and control cells during heat shock using anti-SFA. Time points and sample type (whole cell, pellet or supernatant) are indicated above the bars and from each sample type similar amounts of protein were loaded. A heat shock of 60 minutes duration was applied from T0 to T60. Upper rows: in whole cells only minor variations in the amount of SFA and SFA-GFP were observed during heat shock. Middle rows: analysis of pellets and supernatants of GFP8 cells during heat shock. SFA-GFP was largely removed from the insoluble fraction after the heat shock. Note the difference in apparent molecular weight between soluble and insoluble SFA-GFP. Anti-centrin staining (BAS6.8) of the same samples is shown as a loading control. Lower rows: supernatant and pellet of control cells. Note the shift in molecular weight between soluble and insoluble forms of SFA. wc-c, whole cell control.

necessary for fiber formation. To further determine the region necessary for fiber formation, we expressed a construct coding for a SFA-GFP with a C-terminal deletion of six residues, which showed similar properties to those of ΔC18 (not shown). Next, we exchanged the penultimate serine with either alanine (SFA-GFP-SA) or glutamic acid (SFA-GFP-SE). The latter mimics phosphoserine and resulted in a mostly soluble protein, as documented by western blotting (Fig. 6C, lower panel), and fluorescence microscopy, which showed a dot or small cross near the flagellar base (not shown). By contrast, SFA-GFP-SA was hardly detected in the supernatant obtained from overexpressing strains (e.g. SA11). Fluorescence microscopy of SFA-GFP-SA strains showed large cross-like structures, often with additional branches and additional fibers that were not connected to the

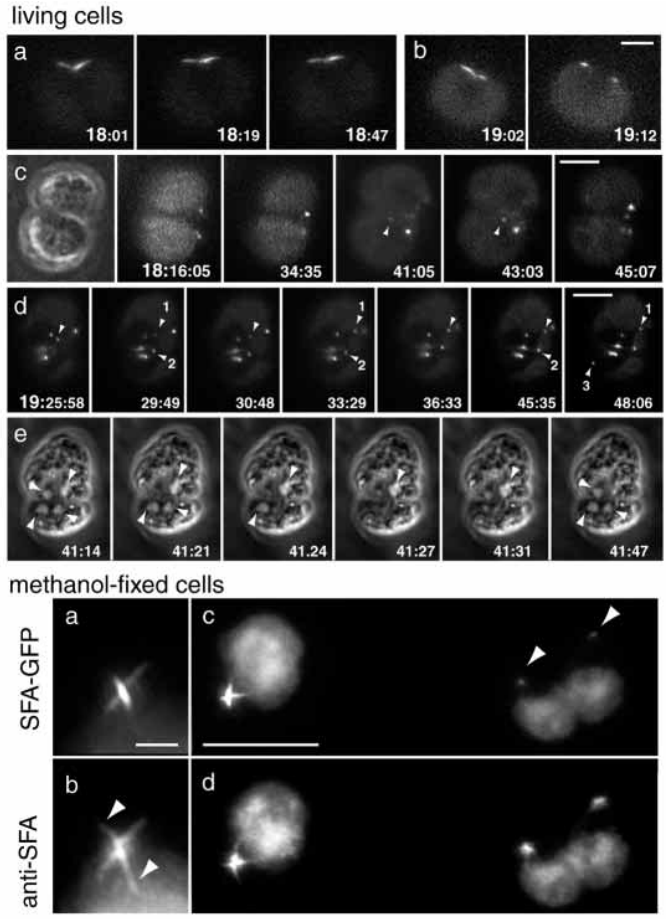

Fig. 5. Observation of SFA-GFP in dividing GFP8 cells. Living cells: the recording time of each picture is indicated (MESZ hours in large numbers; minutes – and in c-e, also seconds – in small numbers). (a,b) Two examples of cells prior to the first division. (c-e) Cells during the first division. (e) Phase contrast images of the cell documented in d showing the four pulsing contractile vacuoles (arrowheads). Arrowhead in c: moving dot of SFA-GFP. Arrowheads in d: #1, rapidly moving dot; #2, slowly moving dot; #3, dot appearing from the back of the cell. Bars, 5 μm (c,d), 4 μm (a,b). Methanol-fixed cells: (a,c) SFA-GFP and corresponding anti-SFA signals (b,d) showing that SFA-GFP is underrepresented in two of the fibers (arrowhead in b) and in dividing cells (arrowheads in c). The differences documented in a/b are characteristic for cells before division and indicate a rapid removal of SFA-GFP from the axis-forming fibers (arrowheads in b) along the two-stranded roots. Bars, 2 μm (a,b), 10 μm (c,d).

basal apparatus or associated with microtubules (Fig. 6D, not shown). Interestingly, the serine-to-alanine mutation conferred heat stability (1 hour, 40°C) to the fibers (Fig. 6D).

SFA-GFP interfered with the expression of SFA

We noted that cytoskeletons isolated from GFP8 cells contained less SFA in comparison to control cells (Fig. 6C). A similar reduction of untagged SFA was noticed in cells expressing the assembly incompetent SFAΔC18-GFP, suggesting that soluble SFA-GFP might repress the expression of SFA. To analyze further the assumed interference between the expression of SFA-GFP and SFA, we took advantage of the observation that SFA-GFP was mostly soluble at higher temperatures: only short fibers were observed by fluorescence microscopy at 32°C, whereas large signals were observed at 25°C and especially at 15°C when fluorescence was often prominent, even along the proximal parts of the four-stranded microtubular roots (Fig. 7A). On western blots of whole cells cultivated at 15, 25 or 32°C, decreasing amounts of SFA-GFP were detected (Fig. 7B). This decrease was caused by a loss of polymeric SFA-GFP, whereas almost constant amounts of SFA-GFP and only traces of SFA were detected in the soluble fractions (Fig. 7C). The results suggest that soluble SFA and SFA-GFP are maintained at constant low levels by degradation, although other explanations are possible. Interestingly, the amount of SFA increased with rising temperatures (Fig. 7B,C), which could represent a mechanism by which cells try to balance the temperature-induced loss of polymeric SFA-GFP. Thus, striated fibers were mostly composed of SFA-GFP at 15 or 25°C but contained more SFA than SFA-GFP at 32°C.

Because cells assemble fibers with different ratios of SFA to SFA-GFP depending on the environmental temperature, temperature shifts should induce synthesis of SFA and degradation of SFA-GFP. Indeed, increased levels of SFA and decreased levels of SFA-GFP could be observed within 6 hours after increasing the temperature from 15 to 32°C (Fig. 8A, lanes 1,5). To test whether SFA was synthesized de novo, we added 2 μM cycloheximide to cells before shifting them to 32°C. In comparison to controls, the cytoskeletons of cells treated with cyclohexmide for 6 hours contained less SFA but more SFA-GFP, which was observed either in cells heat-shocked before the temperature shift to dissolve the fibers (Fig. 8A, lanes 3,4) or in cells only shifted from 15 to 32°C (Fig. 8B, lanes 2,3). We presume that cycloheximde does not only block SFA synthesis but also interferes with the degradation of soluble SFA-GFP. Assuming further a balance between soluble and insoluble SFA-GFP, a block in the degradation of soluble SFA-GFP should force some protein to be re-incorporated into striated fibers in the presence of cycloheximide at 32°C. Accordingly, fluorescent fibers in cells treated with cycloheximide after the temperature shift were larger than in controls without cycloheximide (Fig. 8C, part 1,3). Interestingly, 2 hours after cycloheximide was removed from temperature-shifted cultures, elevated amounts of SFA and SFA-GFP were detected on western blots, and large fibers were observed by fluorescence microscopy (Fig. 8B, lane 4, C4). In cells that were permanently cultivated at 15°C neither cycloheximide treatment nor its removal caused significant changes in the ratio or amount of SFA and SFA-GFP (not shown).

Reduction of SFA expression by RNA interference

We constructed a gene consisting of the 5′ region of the *sfa* gene, including parts of the 5′ UTR and the first two introns, to which the corresponding region of the cDNA was fused in the antisense orientation (Fig. 9A). This construct is predicted to form dsRNA with a hairpin that has been shown to effectively induce post-transcriptional gene silencing in plants (Smith et al., 2000) and *Chlamydomonas* (Fuhrmann et al., 2001). Indeed, western blots with anti-SFA of cells transformed with pCB-AS1 identified strains (five out of 20

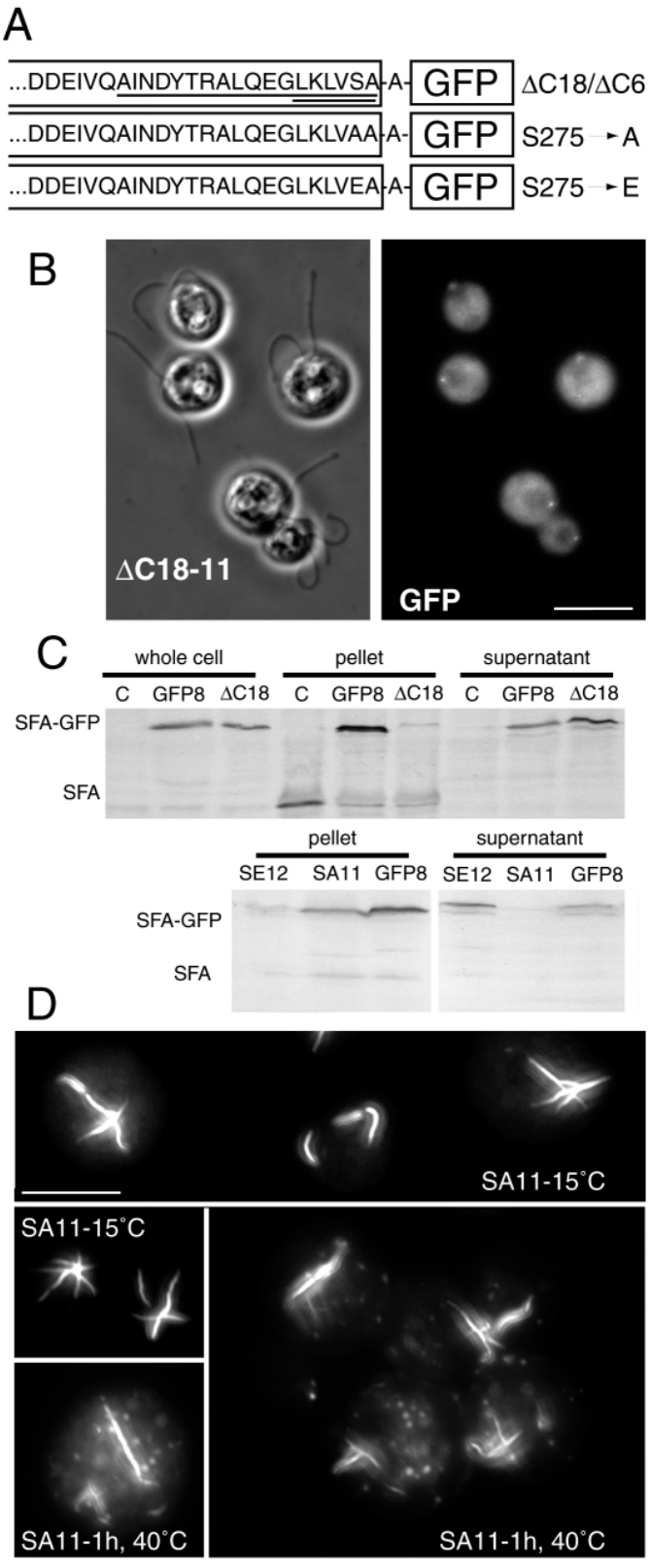

Fig. 6. Analysis of cells expressing GFP-tagged modified SFAs. (A) Sequence of the C-terminal domain of SFA. Underlined residues are truncated in ΔC18; the deletion in ΔC6 is double underlined. Lower rows show the point mutations used to modify the penultimate serine. (B) Phase contrast and fluorescent image of strain ΔC18-11 cells fixed with –20°C methanol. The GFP-tagged protein was concentrated near the basal bodies. Bar, 10 μm. (C) Western blot analysis of strains expressing truncated or mutated SFA molecules using anti-SFA. Upper panel: distribution of SFA, and GFP-tagged SFA or SFAΔC18 in control (C), GFP8 and ΔC18-11 cells. Note the reduced amounts of SFA in GFP8 and Δ18-C11. In the latter, most of the GFP-tagged protein remained in the supernatant, whereas full-length SFA-GFP was mostly insoluble. The amounts loaded in each lane corresponded to 3.6×10^5 cells (whole cell), 1.8×10^6 cells (pellets) and 3.3×10^5 cells (supernatants). Lower panel: comparison of pellets and supernatants from GFP8, SE12 and SA11. Note that most of the SFA-GFP-SE was soluble, whereas SFA-GFP-SA was highly insoluble. Similar amounts of pellets and supernatants were loaded. (D) Fluorescence images of strain SA11 cultivated at 15°C before and immediately after a heat shock of 60 minutes. Note the star-like arranged SFA fibers and the dotted signals after heat shock. Bar, 10 μm.

tested) with significantly reduced amounts of SFA. In two of these cell lines, AS5 and AS8, the expression of the antisense construct was verified by northern blotting, which showed a transcript of ~900 bp in the total RNA isolated from cells 45 minutes after heat shock (Fig. 9B). Furthermore, Southern blotting showed that AS8 contained a single copy of the transformed plasmid (not shown).

The amount of residual SFA varied between cell lines, and for further analyses we chose strains (AS3, AS5, AS6 and AS8) in which SFA was barely detectable on western blots of isolated cytoskeletons (Fig. 9C) and was not detected on westerns of whole cells (not shown). In these cell lines, indirect immunofluorescence with anti-SFA still showed a dotted signal near the basal bodies and, in a few cells, cross-like structures were observed (Fig. 9D). We assume that these signals were caused by residual SFA in the cytoskeletons. Most antisense strains showed elevated numbers of uniflagellate or flagella-less cells, and AS3 had no flagella (Table 1). The latter could be the result of an independent mutantion, for example, caused by insertion of the transformed DNA into a gene necessary for flagellar assembly. In control or GFP8 cells approximately 98% of cells were biflagellate, whereas in the antisense strains only 51- 86% showed wild-type flagellar numbers, which included up to 10% of cells with one fully grown flagellum and one shorter or stumpy flagellum (Fig. 9D). In AS8 cells, flagellar regeneration after mechanical deflagellation was delayed and slow compared with control or GFP8 cells (not shown). Several counts of flagellar numbers in AS5 and AS8 over several months showed a variation in the distribution of cells with zero, one or two flagella (Table 1). On western blots, variable but always significantly reduced amounts of SFA were detected (not shown). We also generated double transformants by introducing pCB740-SFA-GFP into AS5 by cotransformation with pJN4, containing the *cry1* gene, which confers emetine resistance (Nelson et al., 1994). The phenotype of AS5-SFA-GFP transformants was similar to that of AS5 and strains overexpressing SFA-GFP were not detected (Table 1). Fluorescence microscopy revealed weak globular signals scattered in the cytoplasm, in addition to a weak dot at the apical cell pole (Fig. 10A). Western blotting with anti-SFA and anti-GFP revealed that SFA-GFP mostly remained in the 15,300 ***g*** supernatant after cell lysis, when expressed in the AS5 background (Fig. 10B). Presumably, the

Table 1. Flagellar numbers in transformants expressing GFP-tagged SFA or an antisense construct

Number of flagella	C	GFP8	ΔC11	AS3	AS5-1	AS5-2*	AS5-3	AS5-4	AS6-1	AS6-2*	AS8-1	AS8-2	AS8-3	AS8-4	AS5-GFP25	AS5-GFP34
0	1	1	1	100	21	13	6	10	16	12	40	14	29	13	27	21
1	1	1	0	0	28	14	6	5	22	15	4	6	16	21	6	5
2	98	97	98	0	51	72	86	86	62	71	55	80	54	66	67	74
>2	1	1	1	0	0	1	2	0	0	2	1	0	0	0	0	0
n	302	176	138	118	130	105	100	85	100	126	167	114	141	169	163	78

Control cells (C) or GFP8 were mostly biflagellate. Counts of AS5 and AS8 (e.g. AS5-1, -2, -3,...) were distributed over several months. All counts were performed during the first 7 hours of the light cycle. AS5-GFP25 and -GFP34 are double transformants, described in the text.
*Samples from cultures maintained at 15°C.

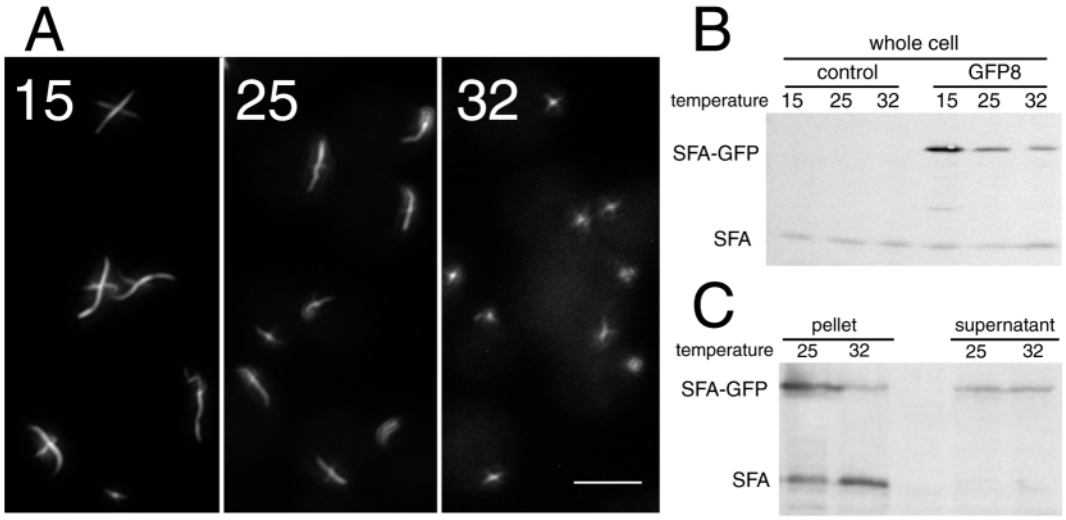

Fig. 7. Effect of environmental temperature on the size and composition of the SMAFs in GFP8 cells. Cells, previously maintained at 15°C, were grown for 48 hours at the temperatures indicated. (A) GFP fluorescence images of cells grown at 15, 25 or 32°C. Bar, 5 μm. (B) Western blot analysis of control and GFP8 cells cultivated at 15, 25 or 32°C with anti-SFA. The amount of SFA-GFP decreased with rising temperatures, whereas slightly more SFA was detected in cells cultivated at 32°C. The amount of SFA in control cells remained almost constant under the conditions chosen. (C) Comparison of insoluble and soluble fractions from GFP8 cells cultivated at 25 or 32°C, revealing higher levels of SFA in the pellet at elevated temperature. Note the constant amount of SFA-GFP in the supernatant of GFP8 cells cultivated at 25 or 32°C. Anti-SFA was used to detect wild-type and GFP-tagged SFA. Similar amounts of whole cells, pellets and supernatants were loaded.

crucial concentration for polymerization of SFA-GFP, which could be much higher than that for SFA, was not reached when expressed in the antisense background.

Discussion

We expressed GFP-tagged SFA in *Chlamydomonas* to facilitate the in vivo analysis of noncontractile striated roots. In principle, SFA-GFP behaved similar to the untagged protein, for example, polymerization into striated fibers and mitotic solubilization of fibers, but we also noted differences that were either caused by the GFP tag itself or by the high expression level of the GFP-tagged protein. The latter resulted in the formation of oversized SMAFs, which did not result in any striking change of morphology of cells. In vivo observations indicated that SMAFs grow slowly, increasing first in length by thread-like projections and then in thickness. Interestingly, SFA-GFP showed a strong preference to assemble along the two-stranded microtubular roots, whereas four SMAFs of more-or-less similar length are present in wild-type cells (Weiss, 1984) and in cells expressing only some SFA-GFP (e.g. GFP8 cultivated in the dark). Thus, cells tend to form a SMAF system similar to that of wild-type cells, but an excess SFA-GFP is deposited preferably along the two-stranded microtubular roots. Post-translational modifications are thought to influence the binding of various proteins to microtubules, for example, the neuronal microtubule-associated protein tau interacts preferably with polyglutamylated tubulin (Boucher et al., 1994). The proximal regions of all four microtubular roots are acetylated (LeDizet and Piperno, 1986), a modification that may be involved in targeting SFA to these microtubules. However, acetylation of tubulin is insufficient to explain the large striated fibers formed along the two-stranded roots in cells overexpressing SFA-GFP. This preference, which is also apparent during reassembly of SMAFs after mitosis (Lechtreck and Silflow, 1997), could be caused by an unidentified specialization of the two-stranded roots, or by the way SMAFs are nucleated. Several experiments point towards a specialized central region of the SMAFs that might function as a nucleation center. A bright dot at the cell apex survived heat-shock-induced disassembly of SFA-GFP fibers and truncated, assembly incompetent SFA-GFP were present in this central region, suggesting high stability and additional bonds for this part of the fiber. Initially, the fibers along the two-stranded roots were described as one continuous fiber because the striation pattern showed no gap in the region between the basal bodies (Goodenough and Weiss, 1978), but optical diffraction analysis revealed that the two half fibers had opposite polarities (Patel et al., 1992). SMAFs are highly regular, paracrystalline structures; overexpression of SFA-GFP could accelerate crystallization – especially along the two-stranded roots where the fibers sit end to end. By contrast, the fibers along the four-stranded roots originate or branch off laterally from the axis-forming fibers.

The C-terminal GFP-tag of SFA conferred temperature

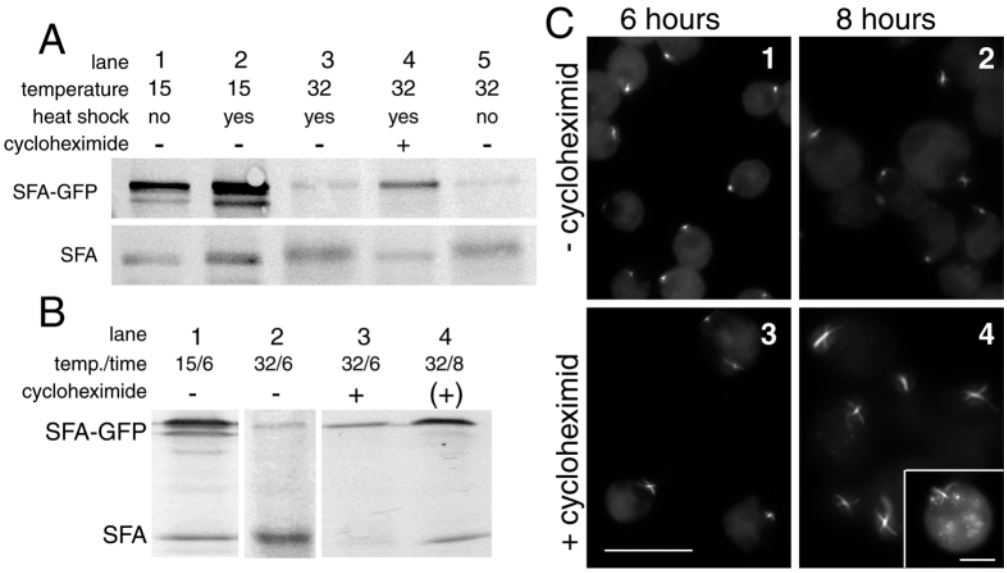

Fig. 8. Effect of cycloheximide on temperature-shifted GFP8 cells. (A) Cells, cultivated at 15°C, were either left untreated (lane 1), heat shocked and incubated at the conditions indicated (lane 2-4), or shifted to 32°C without heat shock (lane 5). After 6 hours, cells were extracted with detergent and the insoluble fractions analyzed by western blotting with anti-SFA. The strong decrease in the amount of SFA-GFP observed after a shift from 15 to 32°C (compare lanes 1 and 5) was partially inhibited by cycloheximide (lane 4). Furthermore, cells treated with cycloheximide (lane 4) contained less wild-type SFA in comparison with controls (lane 3 or 5). (B) Cells, cultivated at 15°C (lane 1), were shifted to 32°C for 6 hours either with (+, lane 3) or without (–, lane 2) cycloheximide. After removal of the cycloheximide (+ in brackets, lane 4), we observed a strong increase in the amount of SFA-GFP, and especially SFA. Temperature and time points are indicated (temp./hours). Anti-SFA was used for detection of SFA and SFA-GFP and similar amounts of cytoskeletons were loaded in lanes 3 and 4. (C) Fluorescence images of GFP8 cells corresponding to the experiment documented in the western blot shown in B. (1) GFP8 cells from a 15°C culture after 6 hours at 32°C; (2) as 1 but two hours later and centrifuged as the sample with cyloheximide; (3) GFP8 cells from a 15°C culture after 6 hours at 32°C in the presence of cycloheximide; (4) as 3, but two hours after cycloheximide has been removed. The cells had assembled long SFA-GFP fibers and some cells contained additional globular aggregates (insert). Bars, 10 μm (overviews) or 5 μm (insert).

sensitivity to the chimeric protein. We assume that GFP, which is about 2.4×4.2 nm in dimension, deformed the C-terminal domain and thereby destabilized SFA-GFP fibers. Constructs with C-terminal deletion of six or 18 residues were mostly soluble, emphasizing the importance of the tail domain for the assembly of striated fibers. The removal of a N- or C-terminal domain, or both, had a severe effect on assembly of certain intermediate filament proteins (for a review, see Heins and Aebi, 1994). We were not able to heat-depolymerize SFA-GFP fibers in vitro, suggesting that the disassembly observed in vivo as a reaction to elevated temperatures was accomplished by cellular factors such as phosphorylation. In vivo, SFA is phosphorylated with a high turnover (Lechtreck and Melkonian, 1991). To test this hypothesis we exchanged Ser275 by either alanine or glutamic acid. The latter mimics phosphoserine and increased the solubility of SFA-GFP. In strains expressing the serine-to-alanine mutation we observed aberrant fiber formation and the mutation conferred heat stability to the polymers. Thus, phosphorylation of Ser275 could regulate the solubility of SFA, a mechanism that could be important to maintain a certain size of the SFA fibers and prevent aberrant fiber formation. Our attempts to express N-terminal truncated SFA molecules, which in vitro are assembly incompetent (Lechtreck, 1998), have failed up to now, indicating that the 5′ UTR or the introns, or both, in the 5′ region of the *sfa* gene are necessary for expression from the HSP70B/rbcS2 fusion promoter (not shown).

SFA-GFP fibers were largely depolymerized before cells enter mitosis, indicating that the mitotic processes dissolving the SMAFs also acted on the GFP-tagged protein. During mitosis SFA-GFP was located in several dot-like structures, and in vivo observations showed rapid and directional movements of these structures with velocities of up to 0.4 μm/minute. Previously, dot-like structures cross-reacting with anti-SFA were observed during cell division of *Chlamydomonas* (Lechtreck and Silflow, 1997). The exact localization and function of the SFA structures outside of the basal apparatus needs to be addressed in future. The results show that GFP tagging is a potent method for the in vivo analysis of cytoskeletal dynamics in *Chlamydomonas*.

Overexpression of SFA-GFP in *Chlamydomonas* caused a decrease in the amount of the wild-type protein. This effect indicated that SFA-GFP expression interfered with the metabolism of SFA. Less SFA was also observed in cells expressing the assembly incompetent tail-less SFA-GFPs. Cells overexpressing full-length SFA-GFP always contained a pool of soluble SFA-GFP. Thus, we assume that soluble SFA-GFP or SFAΔC-GFP downregulates the expression of SFA. The expression of tubulin is also autoregulated: high amounts of soluble tubulin dimers provoke the degradation of mRNAs coding for β-tubulin (for a review, see Cleveland, 1989). In *Chlamydomonas*, the control of SFA expression by the soluble protein could downregulate synthesis before mitosis when SMAFs are depolymerized, or in early interphase when SMAFs have reached a sufficient length. However, the assumed feed back of soluble SFA/SFA-GFP on the expression of SFA is insufficient to explain all effects observed during experiments manipulating fiber length and composition. After shifting cells to elevated temperatures, which caused shrinkage of the SFA-GFP fibers, the amounts of soluble SFA-GFP remained more or less constant, but the amount of SFA in the fibers increased. One possible explanation for this effect is that the temperature-dependent disassembly of the fibers dominated by SFA-GFP liberates binding sites for constitutively expressed SFA. Alternatively, fiber depolymerization would induce the expression of SFA to ensure SMAFs of a certain minimal length. This model would need a mechanism by which cells sense the insufficient size, length or state of the SMAFs. The presence of cycloheximide during a

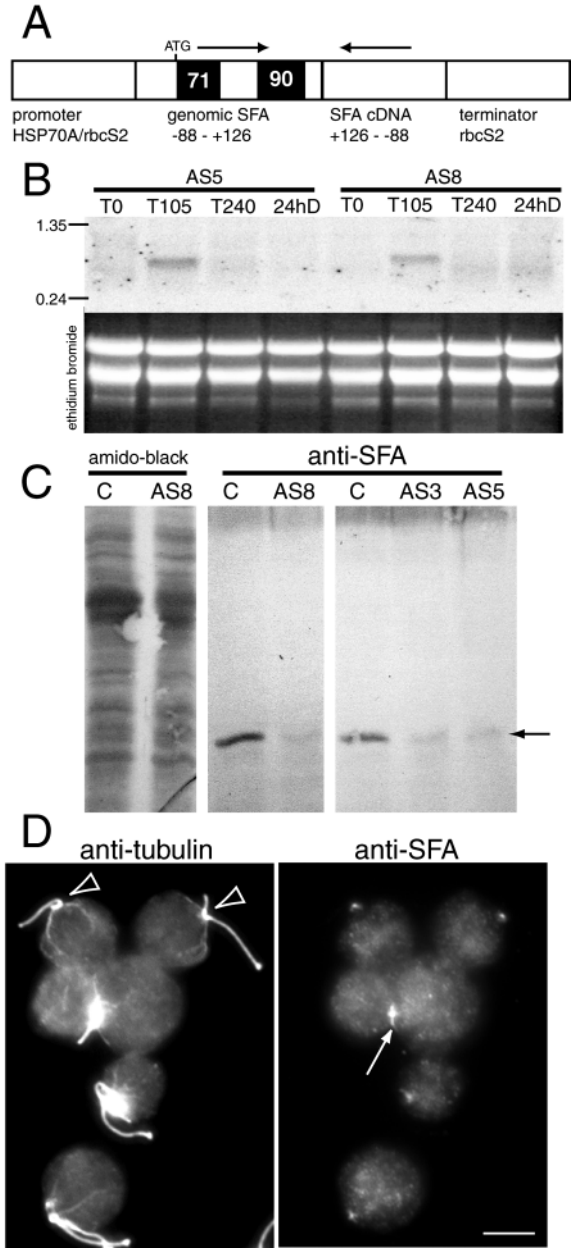

Fig. 9. Characterization of *Chlamydomonas* cells transformed with pCB-AS1. (A) The construct used to reduce the expression of SFA. The solid bars represent introns of 71 bp at +4 and of 90 bp at +91; genomic and complementary DNA of SFA were joined 35 bp after the second intron. (B) Nothern blot documenting the expression of the antisense construct in AS5 and AS8. A transcript of ~900 bp was detected in cells 45 minutes after a heat shock of 60 minutes (T105). The transcript was not detected before (T0) or 3 hours after heat shock (T240), or in a sample isolated from cells maintained in the dark for 24 hours (24hD). Equal amounts of total RNA (~30 μg) were loaded as documented by the ethidium bromide-stained gel. (C) Western blots of control (C) cells and various AS-strains. Equal amounts of cytoskeletons isolated from AS8 and control cells were loaded and stained either with amidoblack (left membrane strip) or probed with anti-SFA (middle membrane strip). Right: membrane strip comparing SFA in insoluble fractions from AS3 and AS5 with that of control cells. Prolonged development of membrane strips visualized some residual SFA in the antisense strains (arrow). (D) AS8 cells permeabilized with –20°C methanol and stained with anti-tubulin (6-11B-1) and anti-SFA. Open arrowheads: uniflagellate cells; arrow: stronger SFA signal. Bar, 5 μm.

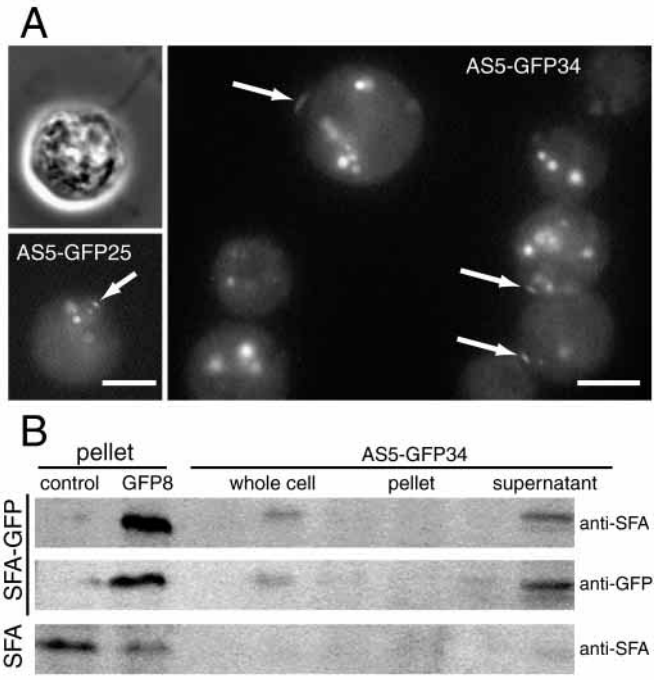

Fig. 10. Expression of SFA-GFP in *Chlamydomonas* AS5 cells. (A) Phase contrast and fluorescent images of AS5-GFP25 and AS5-GFP34 cultivated at 25°C. The cells contained globular aggregates, in addition to a slightly elongated signal near the cell apex (arrows). Both signals were comparably weak. (B) Western blots stained with anti-SFA (top, bottom) or anti-GFP (middle) of whole cells, cytoskeletons, and supernatant of AS5-GFP34 cells. SFA-GFP was detected almost exclusively in the soluble fraction of AS5-GFP34 cells. Note the reduced amounts of wild-type SFA in GFP8 and especially AS5-GFP34 when compared with controls (bottom).

fiber-destabilizing temperature shift resulted not only in lower amounts of SFA but also caused higher levels of SFA-GFP and longer polymers. We suppose that cycloheximide indirectly delayed the degradation of soluble SFA-GFP, which could cause the assembly of longer SMAFs – even at elevated temperatures – because of an equilibrium between soluble and insoluble forms of SFA-GFP. After the removal of the drug, we observed a boost in the expression of SFA and SFA-GFP. It has been shown previously that cycloheximide interferes with stability of mRNAs coding for tubulin (Pachter et al., 1987). In *Chlamydomonas* the drug prevents the degradation of transcripts coding for α-tubulin that accumulate after deflagellation (Baker et al., 1989). The effect of cycloheximide on mRNAs coding for SFA is not known. Our data indicate that the length of the SMAFs depends on a regulatory pathway controlling SFA synthesis, degradation, and the equilibrium between polymerization and depolymerization.

Despite the presence of oversized SMAFs, GFP8 cells had no obvious phenotype (that is, growth, cell size and shape, flagellar position and number, and swimming behavior as observed by light microscopy were indistinguishable from controls), qualified by the observation that cultures of GFP8 maintained at

15°C often contained elevated numbers (~2-9%) of quadriflagellate cells compared with controls (not shown). Furthermore, SFAΔC-GFP did not cause a dominant negative effect as observed for truncated keratin molecules, for example (for a review, see Fuchs, 1995). To explore SFA function, a partial cDNA of SFA was fused in antisense orientation behind the corresponding region of the genomic DNA and expressed to induce gene silencing via the formation of dsRNA, as recently described in *Chlamydomonas* (Fuhrmann et al., 2001). Indeed, we identified cell lines with severely reduced amounts of SFA that often had less than two flagella. The observed phenotype of the antisense strains indicated that SFA or the SMAFs are necessary for flagella assembly or maintenance, or both. Microtubules serve as track for intracellular transport and thus the microtubular roots, which terminate near the basal bodies, could function as supply lines for flagella precursors (Porter et al., 1999). This transport could somehow depend on the SMAFs, which are attached to the flagellar root microtubules. Furthermore, we observed microtubules terminating laterally on the oversized SMAFs of GFP8 cells, and SMAFs of the colorless green alga *Polytomella* function as microtubule organizing centers in vitro (Stearns et al., 1976). However, antibodies for acetylated tubulin and α-tubulin did not identify significant structural changes in the microtubular cytoskeleton of antisense strains as visible by indirect immunofluorescence, but the distribution of γ-tubulin was altered in the strains expressing SFA-GFP and SFA antisense: GFP8 cells often showed anti-γ-tubulin staining along the large SFA-GFP fibers, whereas in AS8 the γ-tubulin signals were smaller than in wild-type cells (K.-F.L., unpublished). Although many molecular details remain to be elucidated, reduced expression levels of SFA might alter the microtubular system near the basal bodies, which could hinder the transport of flagellar proteins. Similar functions could also be valid for similar noncontractile rootlets, which are common in flagellate cells over a broad range of species.

We thank Carolyn Silflow and Pete Lefebvre (University of Minnesota, St Paul, MN) for advice during the isolation of the genomic clone of SFA, plasmids and helpful discussions; Peter Beech (Deakin University, Australia) for critical reading of the manuscript; Michael Schroda and Christoph Beck (Universität Freiburg, Germany) for providing the pCB740 plasmid; and Stefan Geimer and Michael Melkonian (University of Cologne, Germany) for providing anti-γ-tubulin. This study was supported by the Deutsche Forschungsgemeinschaft.

References

Ausubel, F. M., Brend, R., Kingston, R. E., Moore, D. D., Seidman, J. G., Smith, I. A. and Stuhl, K. (1995). *Short Protocols in Molecular Biology*. 3rd edn. New York: Wiley.

Baker, E. J., Diener, D. R. and Rosenbaum, J. L. (1989). Accelerated poly(A) loss on a-tubulin mRNAs during protein synthesis inhibition in *Chlamydomonas*. *J. Mol. Biol.* **207**, 771-781.

Boucher, D., Larcher, J. C., Gros, F. and Denoulet, P. (1994). Polyglutamylation of tubulin as a progressive regulator of in vitro interactions between the microtubule-associated protein Tau and tubulin. *Biochemistry* **33**, 12471-12477.

Church, G. M. and Gilbert, W. (1984). Genomic sequencing. *Proc. Natl. Acad. Sci. USA* **81**, 1991-1995.

Cleveland, D. W. (1989). Autoregulated instability of tubulin mRNAs: a novel eukaryotic regulatory mechanism. *Curr. Opin. Cell Biol.* **1**, 10-14.

Fuchs, E. (1995). Keratins and the skin. *Annu. Rev. Cell Dev. Biol*. **11**, 123-153.

Fuhrmann, M., Oertel, W. and Hegemann, P. (1999). A synthetic gene coding for the green fluorescent protein (GFP) is a versatile reporter in *Chlamydomonas reinhardtii*. *Plant J*. **19**, 353-361.

Fuhrmann, M., Stahlberg, A., Govorunova, E., Rank, S. and Hegemann, P. (2001). The abundant retinal protein of the *Chlamydomonas* eye is not the photoreceptor for phototaxis and photophobic responses. *J. Cell Sci.* **114**, 3857-3863.

Goodenough, U. W. and Weiss, R. L. (1978). Interrelationships between microtubules, a striated fiber, and the gametic mating structure of *Chlamydomonas reinhardi*. *J. Cell Biol.* **76**, 430-438.

Gorman, D. S. and Levine, R. P. (1965). Cytochrome f and plastocyanin: their sequence in the photosynthetic electron transport chain *of Chlamydomonas reinhardi*. *Proc. Natl. Acad. Sci. USA* **54**, 1665-1669.

Heins, S. and Aebi, U. (1994). Making heads and tails of intermediate filament assembly, dynamics and networks. *Curr. Opin. Cell Biol*. **6**, 25-33.

Holberton, D., Baker, D. A. and Marshall, J. (1988). Segmented alpha-helical coiled-coil structure of the protein giardin from the *Giardia* cytoskeleton. *J. Mol. Biol.* **204**, 789-795.

Kindle, K. L. (1990). High-frequency nuclear transformation of *Chlamydomonas reinhardtii*. *Proc. Natl. Acad. Sci. USA* **87**, 1228-1232.

Lechtreck, K.-F. (1998). Analysis of striated fiber formation by recombinant SF-assemblin in vitro. *J. Mol. Biol.* **279**, 423-438.

Lechtreck, K.-F. and Melkonian, M. (1991). Striated microtubule-associated fibers: identification of assemblin, a novel 34-kD protein that forms paracrystals of 2-nm filaments in vitro. *J. Cell Biol.* **115**, 705-716.

Lechtreck, K.-F. and Silflow, C. D. (1997). SF-assemblin in *Chlamydomonas*: sequence conservation and localization during the cell cycle. *Cell Motil. Cytoskeleton* **36**, 190-201.

Lechtreck, K.-F. and Melkonian, M. (1998). SF-assemblin, striated fibers, and segmented coiled coil proteins. *Cell Motil. Cytoskeleton* **41**, 289-296.

Lechtreck, K.-F. and Geimer, S. (2000). Distribution of polyglutamylated tubulin in the flagellar apparatus of green flagellates. *Cell Motil. Cytoskeleton* **47**, 219-235.

LeDizet, M. and Piperno, G. (1986). Cytoplasmic microtubules containing acetylated alpha-tubulin in *Chlamydomonas reinhardtii*: spatial arrangement and properties. *J. Cell Biol.* **103**, 13-22.

Nelson, J. A., Savereide, P. B. and Lefebvre, P. A. (1994). The CRY1 gene in *Chlamydomonas reinhardtii*: structure and use as a dominant selectable marker for nuclear transformation. *Mol. Cell. Biol*. **14**, 4011-4019.

Pachter, J. S., Yen, T. J. and Cleveland, D. W. (1987). Autoregulation of tubulin expression is achieved through specific degradation of polysomal tubulin mRNAs. *Cell*. **51**, 283-292.

Patel, H., Lechtreck, K.-F., Melkonian, M. and Mandelkow, E. (1992). Structure of striated microtubule-associated fibers of flagellar roots. Comparison of native and reconstituted states. *J. Mol. Biol.* **227**, 698-710.

Pitelka, D. R. (1969). Fibrillar systems in protozoa. *Res. Protozool*. **3**, 279-388.

Porter, M. E., Bower, R., Knott, J. A., Byrd, P. and Dentler, W. (1999). Cytoplasmic dynein heavy chain 1b is required for flagellar assembly in *Chlamydomonas*. *Mol. Biol. Cell* **10**, 693-712.

Reize, I. B. and Melkonian, M. (1989). A new way to investigate living flagellated/ciliated cells in the light microscope: immobilization of cells in agarose. *Bot. Acta* **102**, 145-151.

Schiebel, E. and Bornens, M. (1995). In search of a function for centrins. *Trends Cell Biol*. **5**, 197-201.

Schnell, R. A. and Lefebvre, P. A. (1993). Isolation of *Chlamydomonas* regulatory gene Nit2 by transposon tagging. *Genetics* **134**, 737-747.

Schroda, M., Blocker, D. and Beck, C. F. (2000). The HSP70A promoter as a tool for the improved expression of transgenes in *Chlamydomonas*. *Plant J*. **21**, 121-131.

Smith, N. A., Singh, S. P., Wang, M.-B., Stoutjesdijk, P. A., Green, A. G. and Waterhouse, P. M. (2000). Total silencing by intron-spliced hairpin RNAs. *Nature* **407**, 319-320.

Sperling, L., Keryer, G., Ruiz, F. and Beisson, J. (1991). Cortical morphogenesis in *Paramecium*: a transcellular wave of protein phosphorylation involved in ciliary rootlet disassembly. *Dev. Biol*. **148**, 205-218.

Stearns, M. E., Connolly, J. A. and Brown, D. L. (1976). Cytoplasmic microtubule organizing centers isolated from *Polytomella agilis*. *Science* **191**, 188-191.

Weber, K., Geisler, N., Plessmann, U., Bremerich, A., Lechtreck, K.-F. and Melkonian, M. (1993). SF-assemblin, the structural protein of the 2-nm filaments from striated microtubule associated fibers of algal flagellar roots, forms a segmented coiled coil. *J. Cell Biol*. **121**, 837-845.

Weiss, R. L. (1984). Ultrastructure of the flagellar roots in *Chlamydomonas* gametes. *J. Cell Sci*. **67**, 133-143.